# Requirement of subunit co-assembly and ankyrin-G for M-channel localization at the axon initial segment

**Hanne B. Rasmussen[1,*], Christian Frøkjær-Jensen[1], Camilla S. Jensen[1], Henrik S. Jensen[1], Nanna K. Jørgensen[1], Hiroaki Misonou[2,3], James S. Trimmer[2], Søren-Peter Olesen[1] and Nicole Schmitt[1]**

[1]Department of Medical Physiology, The Panum Institute, University of Copenhagen, Blegdamsvej 3, DK-2200 Copenhagen N, Denmark
[2]Department of Pharmacology, School of Medicine, University of California, Davis, CA 95616, USA
[3]Department of Biomedical Sciences, Dental School, University of Maryland, Baltimore, MD 21201, USA
*Author for correspondence (e-mail: hannebr@mfi.ku.dk)

*Accepted 9 January 2007*
*Journal of Cell Science 120, 953-963 Published by The Company of Biologists 2007*
*doi:10.1242/jcs.03396*

## Summary

**The potassium channel subunits KCNQ2 and KCNQ3 are believed to underlie the M current of hippocampal neurons. The M-type potassium current plays a key role in the regulation of neuronal excitability; however, the subcellular location of the ion channels underlying this regulation has been controversial. We report here that KCNQ2 and KCNQ3 subunits are localized to the axon initial segment of pyramidal neurons of adult rat hippocampus and in cultured hippocampal neurons. We demonstrate that the localization of the KCNQ2/3 channel complex to the axon initial segment is favored by co-expression of the two channel subunits. Deletion of the ankyrin-G-binding motif in both the KCNQ2 and KCNQ3 C-terminals leads to the disappearance of the complex from the axon initial segment, albeit the channel complex remains functional and still reaches the plasma membrane. We further show that although heteromeric assembly of the channel complex favours localization to the axon initial segment, deletion of the ankyrin-G-binding motif in KCNQ2 alone does not alter the subcellular localization of KCNQ2/3 heteromers. By contrast, deletion of the ankyrin-G-binding motif in KCNQ3 significantly reduces AIS enrichment of the complex, implicating KCNQ3 as a major determinant of M channel localization to the AIS.**

Key words: KCNQ, M current, Epilepsy, Axon initial segment, Ankyrin-G, Targeting

## Introduction

Voltage-gated KCNQ (Kv7) potassium channels are of critical importance in excitable tissue. In the nervous system, KCNQ2/3 channel complexes constitute the molecular correlate of the M-current, a widely studied potassium current that plays a dynamic role in controlling the excitability of both central and peripheral neurons (Brown and Adams, 1980; Wang et al., 1998). Mutations in the KCNQ2 and KCNQ3 genes can lead to benign familial neonatal convulsions (BFNC), a generalized form of epilepsy (Biervert et al., 1998; Charlier et al., 1998; Singh et al., 1998). Current reductions of only 20% have been reported to be disease-causing (Schroeder et al., 1998) and disruption of *KCNQ2* in mice is lethal (Watanabe et al., 2000), which stresses the importance of this channel complex. A conditional knock-out of *KCNQ2* has been reported to show increased neuronal excitability, reduced spike-frequency adaptation, attenuated medium afterhyperpolarization, and reduced intrinsic sub-threshold theta resonance in CA1 neurons of the hippocampus (Peters et al., 2005).

KCNQ2 and KCNQ3 are co-expressed in several neuronal populations including the hippocampus (Cooper et al., 2000; Cooper et al., 2001; Wang et al., 1998). However, reports of the exact subcellular localization of the channel complex have been divergent (Cooper et al., 2000; Cooper et al., 2001; Roche et al., 2002; Shah et al., 2002; Geiger et al., 2006; Weber et al., 2006). Recent studies have reported expression of KCNQ2 and KCNQ3 at nodes of Ranvier and at the initial segment of axons (AIS) of several central and peripheral neurons (Devaux et al., 2004; Pan et al., 2006; Schwarz et al., 2006). If KCNQ2/3 complexes indeed localize to the AIS it would provide the channel with a very strong influence upon neuronal excitability, as it is believed to be the site of integration of synaptic inputs to the neuron and where action potentials are initiated.

The AIS is characterized by a high density of voltage-gated sodium channels ($Na_v$) that are necessary for action potential initiation (Catterall, 1981). It has been demonstrated that the adaptor protein ankyrin-G is important for the localization of $Na_v$ to the AIS (Davis and Bennett, 1994; Kordeli et al., 1995). A targeted knock-out of ankyrin-G expression in the postnatal cerebellum of mice disrupted the clustering of $Na_v$ in the AIS and Purkinje cell neurons from the mutant mice were unable to fire normal action potentials (Jenkins and Bennett, 2001; Zhou et al., 1998). Ankyrin-G thus appears to be a central player in the localization of $Na_v$ at the AIS.

Detailed knowledge concerning the localization of $Na_v$ is emerging. However, little is known concerning the mechanisms governing KCNQ2/3 channel localization. In the present study, we have examined the subcellular expression pattern of KCNQ2 and KCNQ3 in adult rat hippocampus and in primary cultured hippocampal neurons. In addition, using a combined immunocytochemical and electrophysiological approach, we have addressed the targeting and clustering of exogenous

KCNQ2 and KCNQ3 subunits in hippocampal cultures. Here we demonstrate, in agreement with two papers that were published while this paper was in preparation (Pan et al., 2006; Chung et al., 2006), that KCNQ2/3 complexes localize to the AIS through the ankyrin-G-interaction domains in the KCNQ2 and KCNQ3 C-termini. We show that heteromeric assembly of the channel complex favours the localization to the AIS. We furthermore demonstrate that deletion of the ankyrin-G-binding motif in KCNQ2 alone does not alter the subcellular localization of the complex. By contrast, deletion of the motif contained within KCNQ3 leads to a significant reduction in AIS enrichment of the channel complex, implicating KCNQ3 as an important component for M channel localization to the AIS.

## Results

### Subcellular localization of KCNQ2 and KCNQ3 complexes in adult rat hippocampus

As a first step toward characterizing the subcellular localization of KCNQ2 and KCNQ3 subunits in mammalian central neurons, we examined the localization of the two subunits in adult rat hippocampus. Immunolabeling experiments with antibodies directed against KCNQ2 and KCNQ3 demonstrated expression of both channel subunits in the CA1 and CA3 subfields and in the dentate gyrus. In agreement with two recent studies (Devaux et al., 2004; Pan et al., 2006), KCNQ2 and KCNQ3 were primarily localized to the axon initial segment of adult rat hippocampal pyramidal neurons where they co-localized with ankyrin-G (Fig. 1).

### Endogenous expression of KCNQ potassium channels in hippocampal cultures

Since little is known concerning the mechanisms that dictate KCNQ2/3 channel localization, we decided to address this issue in cultured primary hippocampal neurons. First, we looked for possible endogenous expression of KCNQ channels in the cultures by RT-PCR (Fig. 2A). The cultures were tested at 10 days in vitro (DIV), the time at which neurons expressing exogenous KCNQ channels were analyzed in the subsequent experiments.

RT-PCR experiments demonstrated mRNA expression of KCNQ2, KCNQ3, KCNQ4 and KCNQ5 subunits in the cultures similarly to the reports on slightly older hippocampal neurons (P5-7) (Shah et al., 2002). The protein expression of KCNQ2 and KCNQ3 in cultures was examined by western blotting and revealed expression of both KCNQ2 and KCNQ3 (Fig. 2B). For KCNQ4 and KCNQ5 protein expression, no reliable antibodies were available; therefore expression of KCNQ4 and KCNQ5 proteins in the cultures was not studied.

We next examined the subcellular localization of endogenous KCNQ2 and KCNQ3 by immunocytochemistry. Fig. 2C illustrates the distribution pattern of the two channel subunits in 21-day-old cultured neurons. KCNQ2 and KCNQ3 displayed similar localization patterns with expression in the somatic region, proximal dendrites and the AIS, the AIS being defined as a single MAP2-negative process emerging from the soma. Staining of the two subunits was enriched in the AIS compared with the distal axon (Fig. 2C). The localization of the two subunits in the cultures resembled the localization observed in adult rat hippocampus, although a pool of what appeared to be intracellularly localized protein could be detected in the soma.

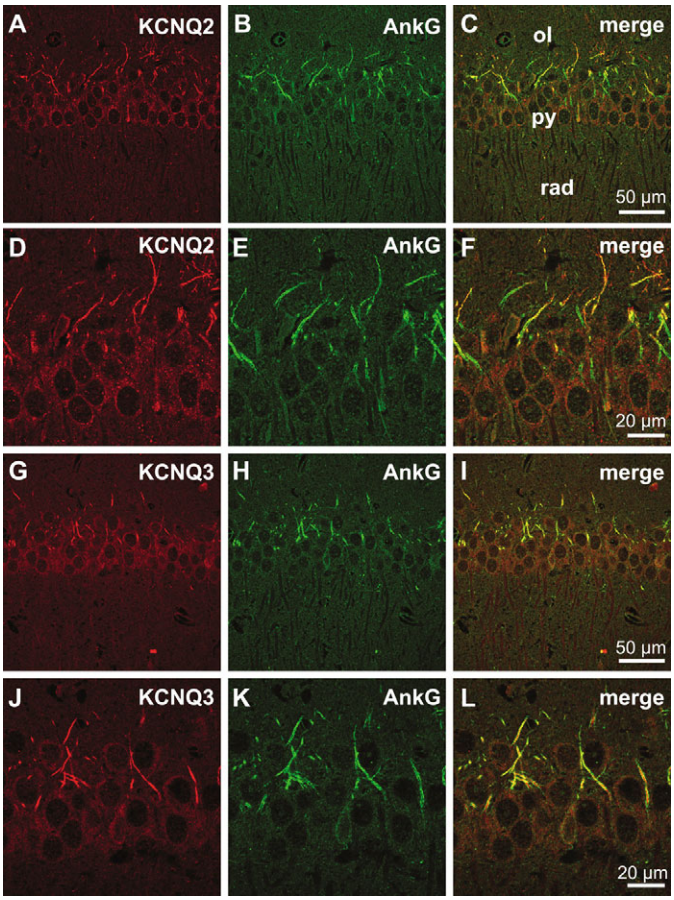


**Fig. 1.** Co-immunolocalization of KCNQ2 and KCNQ3 with ankyrin-G in CA1 of rat hippocampus. (A-F) Cross-section of rat hippocampal CA1 double-labeled for KCNQ2 (A,D) and ankyrin-G (B,E). (G-L) Cross-section of rat hippocampal CA1 double-labeled for KCNQ3 (G,J) and ankyrin-G (H,K). KCNQ2 and KCNQ3 both co-localize with ankyrin-G in this region. Panels D-F and J-L represent a magnified view of the pyramidal cell layer. ol, oriens layer; py, pyramidal cell layer; rad, stratum radiatum.

The presence of endogenous KCNQ channels in cultures was also studied by patch clamp electrophysiology. Using a protocol designed to specifically activate the M-current (Shah et al., 2002) we measured a small, non-inactivating current that could be inhibited by application of the KCNQ-specific blocker XE-991 (Fig. 2D). Thus, the relatively low level of endogenous M-current (1.1±0.4 pA/pF, $n$=8) is in agreement with the presence of endogenous KCNQ channels detected by PCR, western blotting and microscopy.

As we intended to examine the localization pattern of exogenously expressed KCNQ channel subunits in subsequent experiments, we next sought to validate our assay system. We therefore performed western blotting experiments to ascertain relative expression ratios of endogenous versus exogenous KCNQ subunits.

As illustrated in Fig. 2E, hippocampal neurons transfected with cmyc-tagged human KCNQ2 (hKCNQ2-cmyc) expressed KCNQ2 channels in very high amounts compared with non-transfected neurons. Considering the transfection efficiency (only 1-5% of the neurons were transfected), the level of

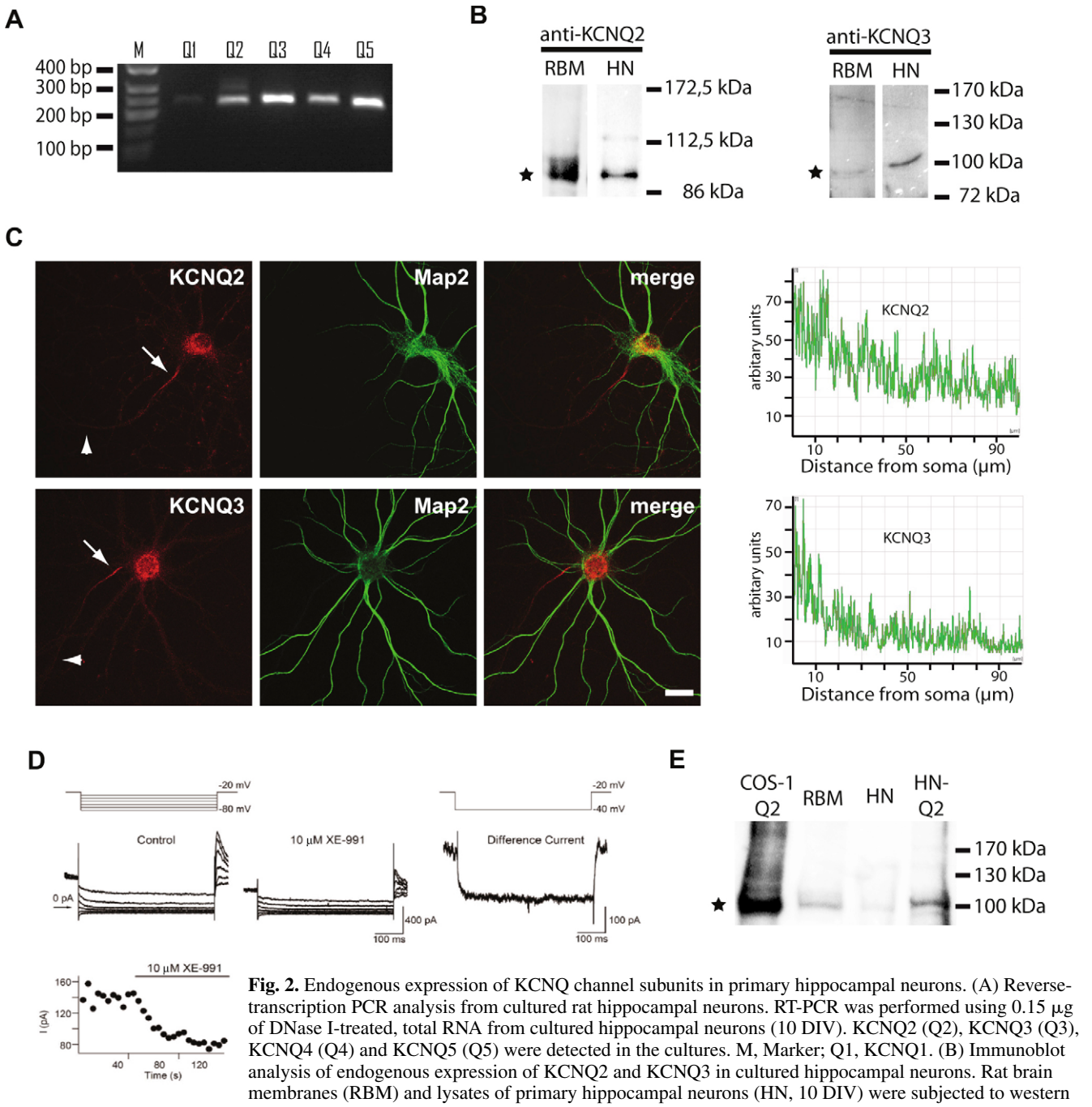


**Fig. 2.** Endogenous expression of KCNQ channel subunits in primary hippocampal neurons. (A) Reverse-transcription PCR analysis from cultured rat hippocampal neurons. RT-PCR was performed using 0.15 μg of DNase I-treated, total RNA from cultured hippocampal neurons (10 DIV). KCNQ2 (Q2), KCNQ3 (Q3), KCNQ4 (Q4) and KCNQ5 (Q5) were detected in the cultures. M, Marker; Q1, KCNQ1. (B) Immunoblot analysis of endogenous expression of KCNQ2 and KCNQ3 in cultured hippocampal neurons. Rat brain membranes (RBM) and lysates of primary hippocampal neurons (HN, 10 DIV) were subjected to western blotting and examined for KCNQ2 and KCNQ3 expression. Stars indicate bands that correspond to KCNQ2 and KCNQ3, respectively. Both channel subunits were detected in the hippocampal cultures. (C) Immunodetection of endogenous KCNQ2 and KCNQ3 in the hippocampal cultures. Hippocampal neurons (21 DIV) were double-labeled for endogenous KCNQ2 and MAP2 or endogenous KCNQ3 and MAP2. Both KCNQ2 and KCNQ3 displayed intracellular, somatic localization as well as localization to the AIS (MAP2-negative). Bar, 20 μm. Arrows mark the position of the AIS, while arrowheads point to the distal axon. (Right) Analysis of the immunofluorescence intensity profiles of endogenous KCNQ2 and endogenous KCNQ3 along the main axon up to 100 μm from the soma from the two images demonstrated that the two subunits were enriched in the AIS compared to the distal axon. (D) Electrophysiological detection of endogenous KCNQ subunits. Shown are currents recorded from a cultured neuron (10 DIV) in the absence (control) and presence of the KCNQ-specific blocker XE-991. Whole-cell currents were recorded from voltage-clamped neurons, and a standard hyperpolarizing protocol (top traces) was used to measure the M-current. Cells were held at –70 mV and then depolarized to –20 mV before they were stepped back to hyperpolarized voltages to measure the M-current. Difference currents were obtained by subtracting the control trace at –40 mV from that in the presence of XE-991. Below is shown a time series of a slowly activating current at –40 mV recorded every 5 seconds in the absence or presence of XE-991. The current is stable in the whole cell recording configuration and is partially blocked by 10 μM XE-991.
(E) Immunoblot detection of KCNQ2 expression in KCNQ2-transfected COS-1 cells (COS-1 Q2), rat brain membranes (RBM), primary hippocampal neurons (HN) and KCNQ2-transfected primary hippocampal neurons (HN-Q2). Note the high level of exogenous KCNQ2 expression compared with the level of endogenous KCNQ2.

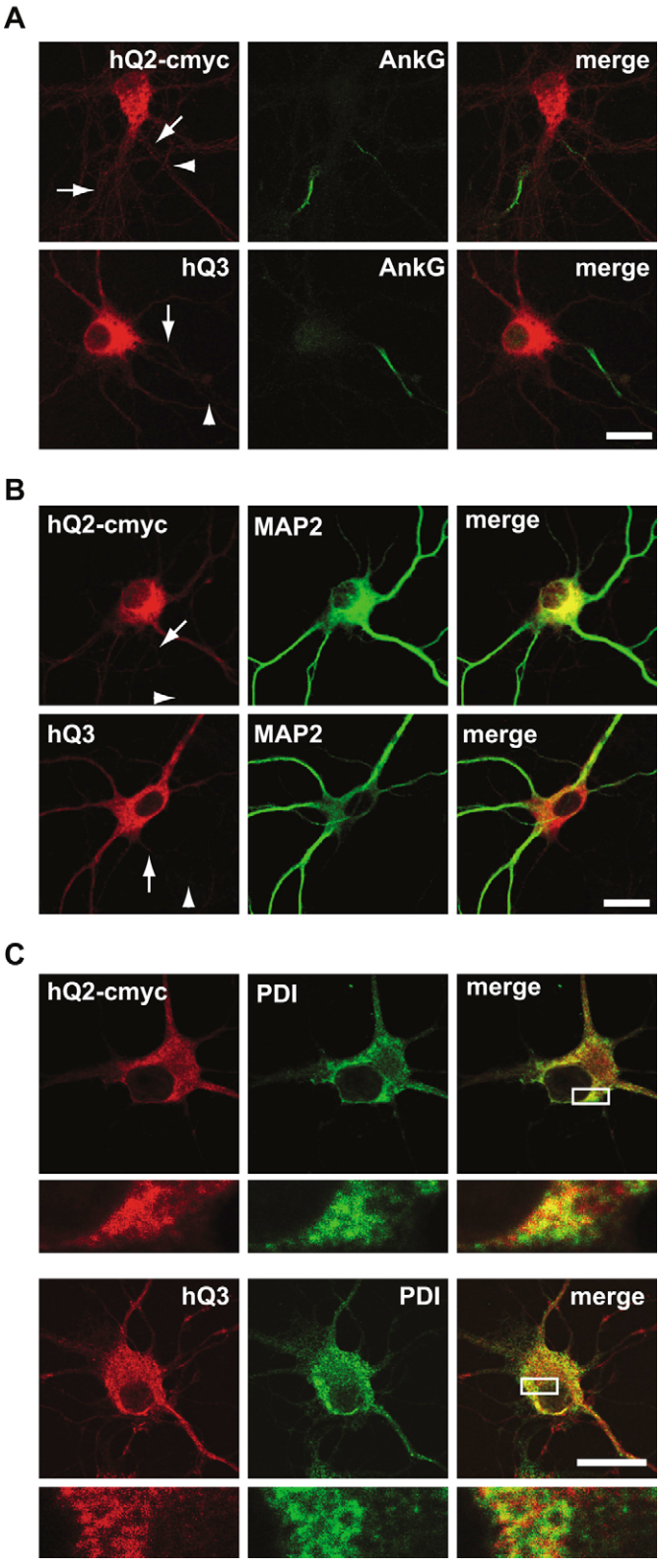


**Fig. 3.** Exogenously expressed hKCNQ2-cmyc and hKCNQ3-FLAG are primarily localized intracellulary in primary hippocampal neurons. Hippocampal neurons expressing hKCNQ2-cmyc (hQ2-myc) or hKCNQ3-FLAG (hQ3). Transfected neurons were fixed and double-labeled with anti-cmyc or anti-hKCNQ3 together with anti-ankyrin-G (AnkG) (A), anti-MAP2 (B) or anti-protein disulfide isomerase (PDI) (C) antibodies. Neither hKCNQ2-cmyc nor hKCNQ3-FLAG displayed a selective enrichment at the AIS (A) and no accumulation of the channel subunits in MAP-2 negative compartments was observed (B). Instead, both subunits displayed a primarily intracellular localization that partly co-localized with the endoplasmic reticulum marker PDI (C). White boxes in the merged images in C represent the magnified regions displayed below. Arrows mark the position of the AIS, while arrowheads point to the distal axon. Bar, 20 μm.

exogenous KCNQ channel protein in transfected neurons greatly exceeds the level of endogenous protein, a finding that was also supported by electrophysiological measurements (Fig. 5B). We therefore decided to proceed with examination of exogenous channel localization under the assumption that KCNQ channel proteins in transfected cells consisted of mainly exogenous channel complexes.

## Exogenous expression of KCNQ2 and KCNQ3 subunits in cultured neurons

We examined the subcellular localization of exogenous hKCNQ2 and hKCNQ3 channels when expressed separately in rat hippocampal cultures. For this purpose differently tagged hKCNQ2 and hKCNQ3 channel constructs were employed. Tagged hKCNQ2-cmyc was detected by anti-cmyc tag antibodies whereas hKCNQ3-FLAG was detected using an anti-KCNQ3 antibody that only recognized exogenous hKCNQ3 but not endogenous rKCNQ3 (data not shown). We did not employ anti-FLAG tag antibodies to detect hKCNQ3, because in our hands the anti-FLAG tag antibodies resulted in high background levels when applied to hippocampal neurons. Interestingly, exogenous hKCNQ2-cmyc and hKCNQ3-FLAG labeling was mainly observed in the somatic region and no selective enhancement of staining in the AIS was detected (Fig. 3A,B). This finding was in sharp contrast to the localization to the AIS observed for endogenous KCNQ2 and KCNQ3 channels. In fact, most hKCNQ2 and hKCNQ3 labeling appeared to be intracellular. Co-labeling with the endoplasmic reticulum (ER) marker PDI demonstrated that part of the exogenous hKCNQ2-cmyc and hKCNQ3-FLAG labeling was localized in the ER (Fig. 3C).

We used patch-clamp electrophysiology to estimate how much exogenously expressed hKCNQ2-cmyc and hKCNQ3-FLAG reached the cell membrane. The electrophysiological measurements supported the notion that hKCNQ3-FLAG exhibits low surface expression. As summarized in Fig. 5B, exogenous expression of hKCNQ3-FLAG resulted in XE991-sensitive currents at levels comparable to those of control neurons (1.4±0.4 pA/pF, $n$=6). However, expression of hKCNQ2-cmyc increased the amount of XE991-sensitive current about sevenfold (6.8±2.4 pA/pF, $n$=6, Fig. 5B). These data agree well with oocyte expression data on the two subunits (Schroeder et al., 1998). Owing to a large variation between cells, the sevenfold current increase observed upon expression of hKCNQ2-cmyc is not significantly different from control conditions ($P$=0.066), but it is likely that a number of KCNQ2 subunits reached the cell surface. Despite an increased number of KCNQ2 channels in the membrane, enrichment at the AIS was not observed (Fig. 5A, AIS/dendrite ratio: 1.0±0.2, $n$=30).

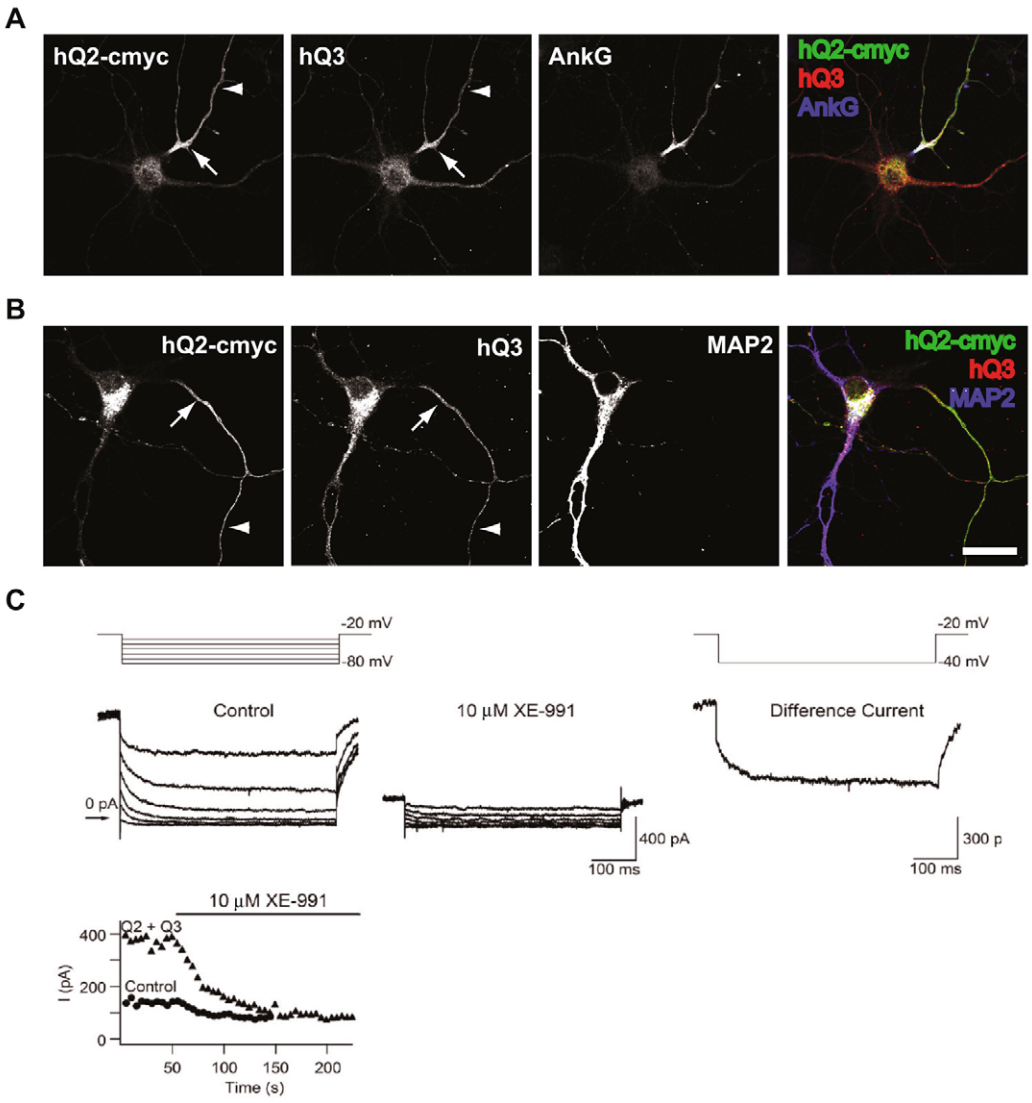


**Fig. 4.** Co-expressed hKCNQ2-cmyc and hKCNQ3-FLAG are localized to the AIS of primary hippocampal neurons. Hippocampal neurons were co-transfected with hKCNQ2-cmyc and hKCNQ3-FLAG, fixed and triple-labeled for hKCNQ2-cmyc, hKCNQ3-FLAG and either ankyrin-G (A) or MAP2 (B). Bar, 20 µm. hKCNQ2-cmyc and hKCNQ3-FLAG labeling was enriched in the AIS, which is positive for ankyrin-G, but devoid of MAP2. Additional staining could also be observed intracellularly as well as in the more distal parts of the axon. Arrows mark the position of the AIS, while arrowheads point to the distal axon. (C) Representative current traces of an hKCNQ2-cmyc/hKCNQ3-FLAG transfected neuron in the absence or presence of 10 µM XE-991. Protocols were as described in Fig. 2. A large, slowly non-inactivating M-current could be measured in transfected neurons. For comparison with the endogenous M-current, the bottom trace shows a time-series of a transfected neuron (Q2+Q3) and a GFP-transfected neuron (Control) before and after application of XE-991 (10 µM). The level of XE-991-sensitive current is on average increased 15-fold in neurons transfected with hKCNQ2-cmyc/hKCNQ3-FLAG compared with that in controls (see Fig. 4B for quantification).

It is well established that the trafficking of KCNQ2 and KCNQ3 is changed upon co-expression of the subunits because the surface expression of both channels is increased upon heteromerization (Etxeberria et al., 2004; Schwake et al., 2000). We examined whether the subcellular localization of hKCNQ2-cmyc and hKCNQ3-FLAG channels was affected by co-expression of the subunits. As shown in Fig. 4, this was indeed the case. Upon co-expression, KCNQ2/3 channel complexes were enriched in a MAP2-negative segment in the proximity of the soma (Fig. 4B). Co-labeling with the AIS marker ankyrin-G demonstrated that KCNQ2-cmyc and KCNQ3-FLAG had redistributed to this compartment (Fig. 4A). To quantify the polarized expression of the KCNQ subunits, we determined the ratio of the mean fluorescence intensity of the proximal axon (0-30 µm from the soma) and compared it with the distal axon (60-90 µm from soma) and the dendrites (Fig. 5A) (Gu et al., 2003). Indeed, this quantification demonstrated an enrichment of staining for the KCNQ2/3 complex in the AIS. The KCNQ2/3 AIS/dendrite ratio was 4.7±0.8 ($n$=30) for hKCNQ2-cmyc and 2.3±0.3 ($n$=30) for KCNQ3-FLAG. This was in contrast to neurons that had been transfected with just one of the two subunits

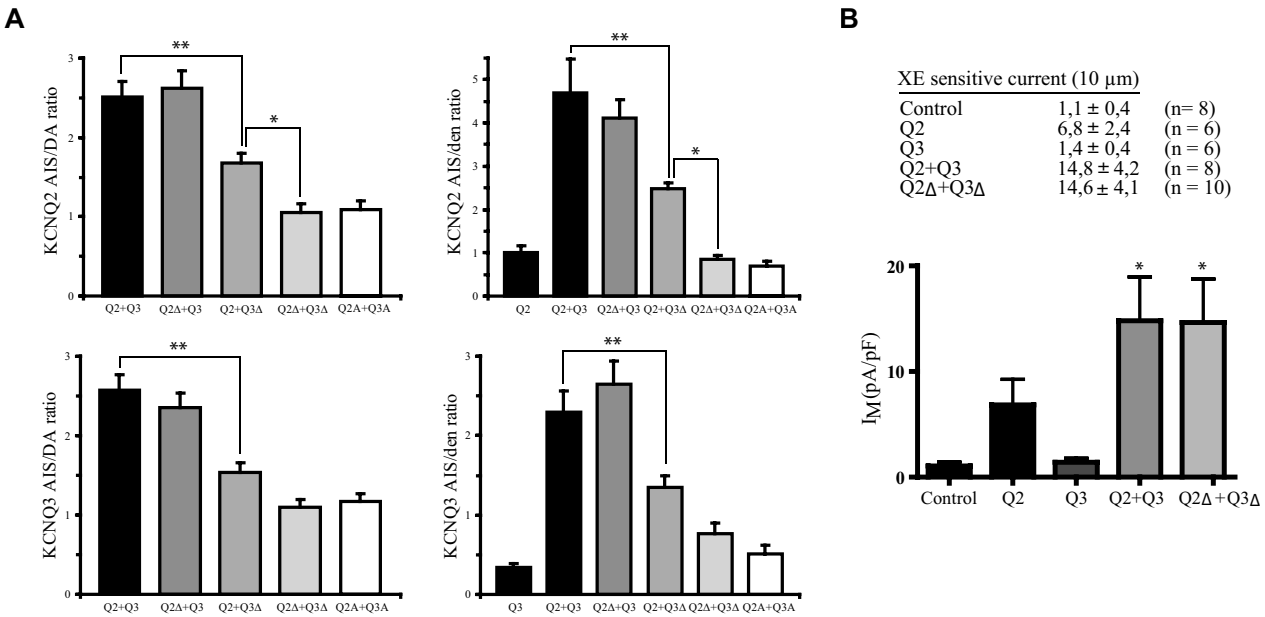


**Fig. 5.** Overview of AIS localization and current levels for the various KCNQ constructs. (A) Summary of observed KCNQ AIS localization in neurons transfected with the listed combinations of constructs. AIS/distal axon (AIS/DA) and AIS/dendrite (AIS/den) ratios were determined for each combination of constructs for 29-30 cells in at least three different cultures. Q2+Q3Δ was statistically different from wild-type Q2+Q3 for both KCNQ2 and KCNQ3 immunofluorescence quantifications, whereas Q2Δ+Q3 was not. In addition, Q2+Q3Δ was statistically different from Q2Δ+Q3Δ in the KCNQ2 quantification, but not for the KCNQ3 quantification. One-way ANOVA and Bonferroni's post-test were used in the comparison of Q2+Q3 vs Q2Δ+Q3, Q2+Q3 vs Q2+Q3Δ and Q2Δ+Q3 vs Q2+Q3Δ (*$P$<0.05, **$P$<0.001). (B) Summary of current density levels observed in neurons transfected with the listed constructs. All neurons were co-transfected with GFP. Recordings were carried out on cultures from at least two different days. Q2+Q3 and ΔQ2+ΔQ3 were statistically different from controls. One-way ANOVA and Dunnet's multiple comparison post-test were used to compare the various constructs with the control (*$P$<0.05). (A+B) Data are displayed as mean±standard error of mean. Abbreviations: control, GFP; Q2, hKCNQ2-cmyc; Q3, hKCNQ3-FLAG; Q2Δ, hKCNQ2-delAnkG; Q3Δ, hKCNQ3-delAnkG; Q2A, Q2-AAA; and Q3-A, Q3-AAA.

(AIS/dendrite ratio: KCNQ2-cmyc: 1.0±0.2 ($n$=30), KCNQ3-FLAG 0.3±0.04 ($n$=29). Co-assembly of KCNQ2 and KCNQ3 subunits therefore appears to favor the localization of the two subunits to the AIS.

Patch clamp measurements supported a redistribution of the two subunits. Increased KCNQ currents could be measured in the co-transfected cells indicating that the surface density of the channel subunits had increased (Fig. 4C). Indeed, a 15-fold increase in XE991-sensitive current density could be detected in cells co-expressing hKCNQ2-cmyc and hKCNQ3-FLAG compared with that in controls (14.8±4.2 pA/pF, $n$=8, Fig. 4C, Fig. 5B).

## KCNQ2 and KCNQ3 localize to the AIS via C-terminal motifs

Since ankyrin-G is required for AIS localization of several proteins including $Na_v$ channels (Garrido et al., 2003; Zhou et al., 1998), we decided to test whether ankyrin-G is also involved in the localization of KCNQ2/3 channel complexes to the AIS.

A conserved ankyrin-G-binding motif has been identified in $Na_v$ channels (Garrido et al., 2003; Lemaillet et al., 2003). Interestingly, similar sequence stretches found in the C-termini of the KCNQ2 and KCNQ3 subunits (Fig. 6A,B) also confer binding to ankyrin-G (Pan et al., 2006). We tested whether these sequences are involved in the AIS localization of KCNQ2/3 complexes. Deletion mutants for KCNQ2 and KCNQ3 were constructed lacking 42 and 47 amino acids from the C-termini, respectively, including deletions of the ankyrin-G-interaction domains (Fig. 6A). The deletion mutant KCNQ2delAnkG and KCNQ3delAnkG complexes were then tested for subcellular localization in hippocampal neurons. When expressed separately, KCNQ2delAnkG and KCNQ3delAnkG did not localize differently from wild-type subunits (data not shown). Also, KCNQ2delAnkG/KCNQ3-FLAG complexes were still targeted to the AIS (Fig. 7A). In fact, AIS enrichment was as efficient for KCNQ2delAnkG/KCNQ3-FLAG complexes as for wild-type heteromeric complexes (Fig. 5A). KCNQ2-cmyc/KCNQ3delankG complexes were also targeted to the AIS (Fig. 7A). However, interestingly, the extent of AIS enrichment was significantly reduced compared with wild-type complexes (Fig. 5A).

Co-expression of KCNQ2delAnkG and KCNQ3delAnkG mutants showed marked differences from co-expression of hKCNQ2-cmyc and hKCNQ3-FLAG. As illustrated in Fig. 7A, deletion of the C-terminal domains of both KCNQ2 and KCNQ3, including the ankyrin-G-binding sequence stretches, abolished AIS enrichment of the complex. The AIS/distal axon ratio for both subunits was reduced to 1. In addition the AIS/dendrite ratio for the subunits was drastically reduced (Fig. 5A).

To verify that the lack of AIS enrichment of the KCNQ2del/KCNQ3del complex was caused by deletion of the ankyrin-G-binding motif in the subunits, point mutations

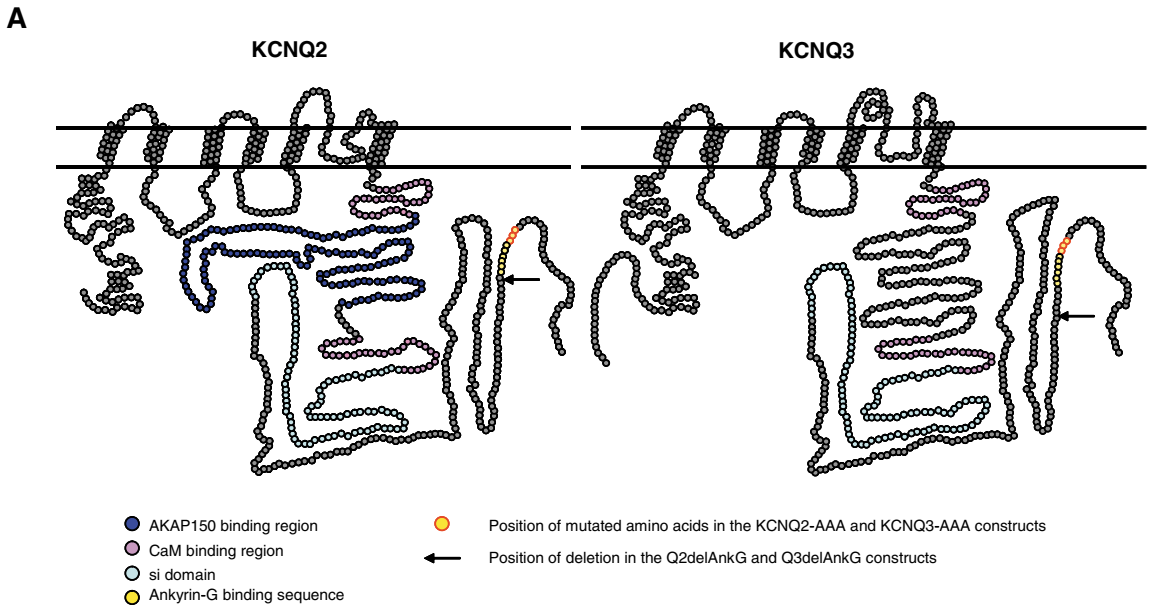


**B**

CLUSTAL W (1.82) multiple sequence alignment

```
hKCNQ2   PYIAEGESD   aa804-812 (Y15065)
hKCNQ3   RYLAEGETD   aa831-839 (NP_004510)
rNav1.6 VPIAVGESD   aa1104-1112 (NP_062139)
           :* **:*
```

**Fig. 6.** The C-termini of KCNQ2 and KCNQ3 contain a potential ankyrin-G-interaction domain. (A) Schematic structure of the KCNQ2 and KCNQ3 subunits with indications of domains of protein-protein interaction. Indicated is also the presence of the ankyrin-G-interaction site in the C-termini of both the KCNQ2 and KCNQ3 subunits. Each circle represents an amino acid. Abbreviations: AKAP, A-kinase anchoring protein, CaM; calmodulin; si, subunit interaction. (B) Clustal W alignment of the 9 amino acid ankyrin-G-binding motif of Nav1.6 along with the ankyrin-G-interaction domain of KCNQ2 and KCNQ3, the corresponding accession no. given in brackets. Red indicates small, hydrophobic residues, blue represents acidic residues, and pink labels basic residues, while green is representative of amino acids containing hydroxyl or amine sidegroups. Asterisks (*) indicate that the residues in that column are identical in all sequences of the alignment; colons (:) indicate that conserved substitutions have been observed.

were introduced in the minimal ankyrin-G-binding sequence (Fig. 6). Specifically, we mutated amino acids demonstrated to be critical for ankyrin-G interaction (Pan et al., 2006), namely KCNQ2-E810A/S811A/D812A (KCNQ2-AAA) and KCNQ3-E837A/T838A/D839A (KCNQ3-AAA). Expression of the mutants KCNQ2-AAA/KCNQ3-AAA also abolished AIS enrichment of the channel complex (Fig. 5A, Fig. 7A). This experiment confirms the mechanism of KCNQ2/3 AIS enrichment to be through the ankyrin-G-binding motif.

The lack of KCNQ2/3 channels at the AIS could either be due to a specific defect in targeting or a more generalized defect in channel subunit interaction or folding. To control for generalized channel defects we did patch clamp experiments on cells co-transfected with C-terminal truncated KCNQ2delAnkG and KCNQ3delAnkG channels. These experiments revealed robust XE-991-sensitive currents at levels comparable with those of hKCNQ2-cmyc/hKCNQ3-FLAG complexes (14.6±4.1 pA/pF, $n$=10, Fig. 5B, Fig. 7B). Thus, the truncated channel subunits were still functional and targeted to the plasma membrane; however, enrichment of the AIS was abolished.

## Discussion

Several studies now point towards an AIS localization of the KCNQ2/KCNQ3 potassium channel complex in central and peripheral neurons. In this study we have examined the subcellular localization of KCNQ2 and KCNQ3 channels in adult rat hippocampal slices and primary hippocampal neurons (Fig. 1). In both cases, we detect the two channel subunits in the AIS of the pyramidal cells. Two recent papers have reported localization of KCNQ2 and KCNQ3 in the AIS of hippocampal neurons of rat and mouse (Devaux et al., 2004; Pan et al., 2006). Our data thus agree well with these observations. Specific KCNQ2 and KCNQ3 localization to the AIS is supported by the fact that we employ primary antibodies to detect the two channel subunits that are different from those used by Devaux et al. (Devaux et al., 2004) and Pan et al. (Pan et al., 2006). In the primary hippocampal cultures, however, Chung et al. report no enrichment of endogenous KCNQ2 and KCNQ3 in the AIS (Chung et al., 2006). Furthermore, Shah et al. report KCNQ2 and KCNQ3 subunits in the somatodendritic membrane of hippocampal pyramidal cells in culture (Shah et al., 2002). The reason for these discrepancies remains unclear.

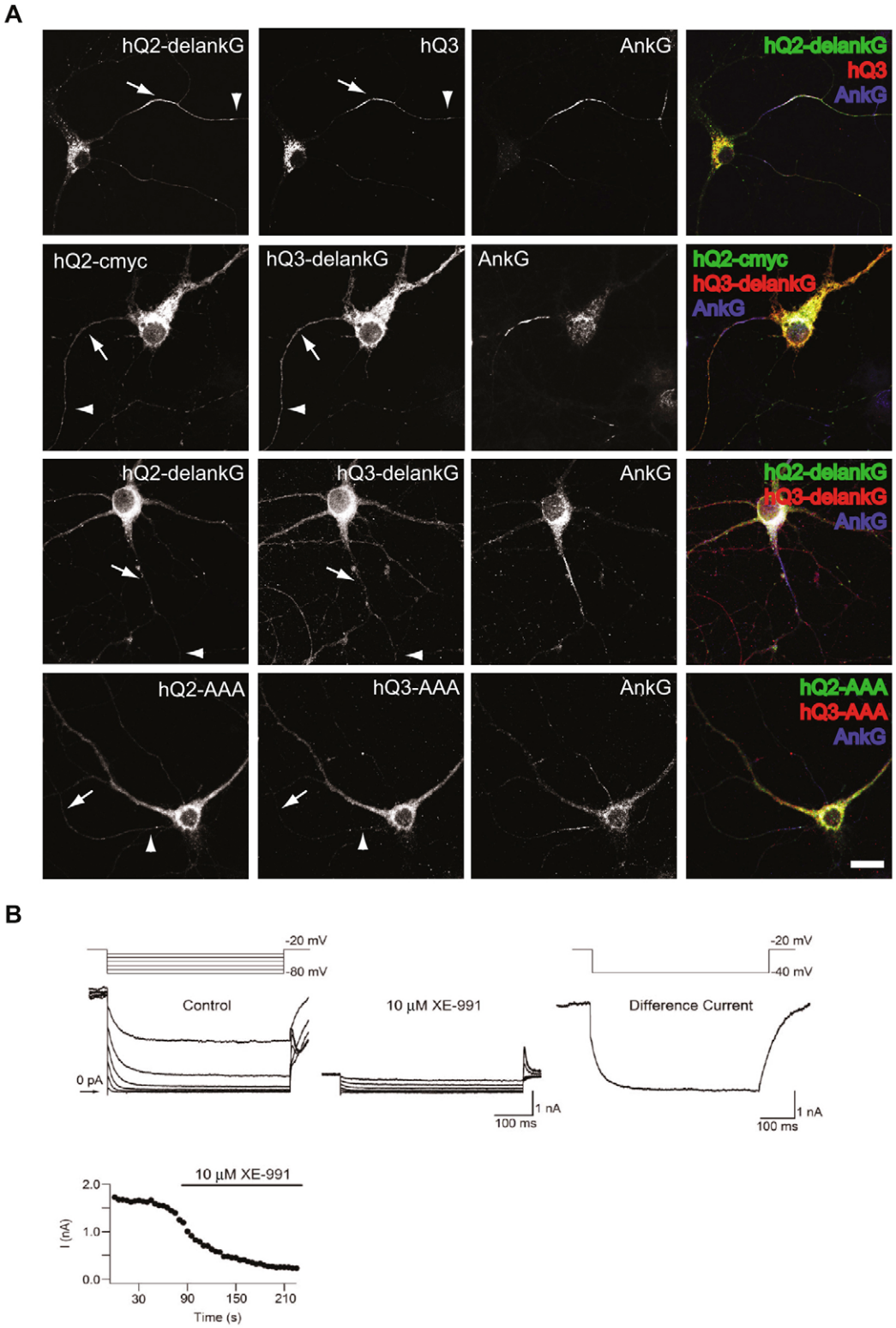


**Fig. 7.** The ankyrin-G-interaction domain mediates retention of KCNQ2/3 complexes at the AIS. (A) Hippocampal neurons were co-transfected with hKCNQ2-delAnkG (Δ803-844) (hQ2-delAnkG) + hKCNQ3-FLAG (hQ3), hKCNQ2-cmyc (hQ2-cmyc) + hKCNQ3-delAnkG (Δ826-872) (hQ3-delAnkG), hKCNQ2-delAnkG + hKCNQ3-delAnkG, or KCNQ2-E810A/S811A/D812A (KCNQ2-AAA) and KCNQ3-E837A/T838A/D839A (KCNQ3-AAA). The cells were fixed and triple-labeled for hKCNQ2, hKCNQ3 and ankyrin-G. Bar, 20 μm. hKCNQ2-delAnkG/hKCNQ3-FLAG were enriched at the AIS to the same extent as wild-type hKCNQ2/hKCNQ3. For hKCNQ2-cmyc/hKCNQ3-delAnkG complexes a significant reduction in the AIS enrichment was observed (see also Fig. 5). For hKCNQ2-delAnkG/hKCNQ3-delAnkG and hKCNQ2-AAA/hKCNQ3-AAA complexes AIS enrichment was abolished. (B) Representative current traces of a hKCNQ2-delAnkG/hKCNQ3-delAnkG transfected neuron in the absence or presence of 10 μM XE-991. Protocols were as described in Fig. 2. Current levels were comparable with those observed for full-length KCNQ2-cmyc/KCNQ3-FLAG transfected neurons, thus the hKCNQ2-delAnkG/hKCNQ3-delAnkG complex is still trafficked to the cell surface.

A localization of KCNQ2/3 channel complexes to the AIS is interesting. First, placing the channels here would provide them with a great impact upon neuronal excitability as they would be able to shunt strong excitatory input when open. This central localization of the channel complex could possibly also explain the fact that a mere 20% current reduction has been reported for BFNC KCNQ2 mutations (Schroeder et al., 1998). Second, KCNQ2/3 channels are heavily regulated by metabotropic receptors (Delmas and Brown, 2005). In fact a large number of receptors have been reported to inhibit the current. Activation of muscarinic, angiotensin II, serotonin, substance P, bradykinin and gonadotropin-releasing hormone receptors all inhibit the KCNQ2/3 current and lead to increased neuronal excitability (Brown and Adams, 1980; Colino and

Halliwell, 1987; Cruzblanca et al., 1998; Shapiro et al., 1994; Simmons et al., 1994). This metabotropic regulation of the KCNQ2/3 complex thereby allows for a fine-tuning of the frequency of action potentials as well as for changing the threshold for firing at the level of the AIS.

To delineate the mechanisms that localize KCNQ2/3 channels to the AIS, we analyzed the subcellular localization pattern of exogenously expressed KCNQ2 and KCNQ3 channels in primary hippocampal neurons. We find that both channels are localized primarily intracellularly when expressed alone (Fig. 3). Co-immunolabeling with an ER marker demonstrated that separately expressed KCNQ2 and KCNQ3 subunits partly localize to this compartment. We interpret this as an indication that under these conditions the homomeric channels are retained in the ER. However, electrophysiological analysis of the transfected cells demonstrated that, in contrast to KCNQ3 homomers, some KCNQ2 homomers appear to reach the plasma membrane. Interestingly, KCNQ2 homomers do not accumulate at the AIS (Fig. 3). The lack of detectable KCNQ2 and KCNQ3 immunofluorescence at the AIS is in good agreement with a recent paper examining KCNQ2/3 surface expression (Chung et al., 2006). Chung et al. exogenously expressed KCNQ2 and KCNQ3 separately in hippocampal neurons and reported low surface expression and no apparent localization of the homomers to the AIS (Chung et al., 2006). Our electrophysiological data suggest that KCNQ2 homomers possibly display some surface expression, although the expression is not concentrated at the AIS. These data stress the importance of employing several strategies to analyze the subcellular localization and surface expression of ion channels.

Co-expression of KCNQ2 and KCNQ3 subunits alters the subcellular localization pattern; KCNQ2/3 heteromeric channels now localize to the AIS (Fig. 4). Concurrently, current levels are increased. Surface expression as well as targeting of KCNQ2 and KCNQ3 channels to the AIS is therefore favored by the co-expression of the two subunits. Like $Na_v$ channels, KCNQ2/3 complexes localize to the AIS through an ankyrin-G-interaction domain (Figs 6, 7) (Chung et al., 2006; Pan et al., 2006). Our electrophysiological analysis of neurons expressing KCNQ2delAnkG/KCNQ3delAnkG complexes demonstrates that although the ankyrin-G-interaction domain is required for localization of the complex to the AIS, it is not required for surface expression. The observed effects of the deletion and point mutations in the KCNQ subunits are therefore likely to result from defective axonal expression and/or AIS accumulation. It was recently demonstrated that the ankyrin-G-binding motif is not required for axonal targeting of the channel complex (Chung et al., 2006), as axonal targeting is also mediated through the membrane proximal domain and amino acids 501-579 of the KCNQ2 C-terminus (Chung et al., 2006). These data agree well with the fact that we observe KCNQ2/3 labeling in the more distal parts of the axon when expressing the truncated KCNQ channel subunits (Fig. 7).

Interestingly, the co-assembly of KCNQ2 and KCNQ3 favors the localization of the complex to the AIS (Fig. 5). However, deletion of the ankyrin-G-binding motif in KCNQ2 alone has no effect upon the polarized localization of the KCNQ2/3 complex. We do, in contrast, observe a significant decrease, but not abolishment, of KCNQ2/3 AIS enrichment when the ankyrin-G-binding motif in KCNQ3 is deleted (Fig. 5A, Fig. 7A). These findings indicate that the ankyrin-G-binding motif in KCNQ3 is important for enrichment of the KCNQ2/3 complex to the AIS. Chung et al. reported that fusion of the C-terminal tail of KCNQ2 (CD4-Q2) to the uniformly distributed protein CD4 resulted in preferential targeting of the fusion protein to the axon and enrichment at the AIS (Chung et al., 2006). Fusion of the KCNQ3 C-terminal tail to CD4 (CD4-Q3) exclusively enriched the fusion protein at the AIS. Also, the AIS enrichment of the CD4-Q3 protein was three to four times more efficient than the CD4-Q2 protein (Chung et al., 2006). Their data therefore also indicate that KCNQ3 more efficiently mediates AIS localization than KCNQ2 does. We speculate that upon deletion of the ankyrin-G-binding motif in KCNQ3, the localization of the KCNQ2/3 complex is dictated by KCNQ2, leading to a decrease in the AIS/distal dendrite ratios.

As pointed out above, AIS localization can be achieved in heteromeric channel complexes in which just one subunit contains the motif, although the motif in KCNQ2 is less effective than the motif in KCNQ3 (Fig. 5B, Fig. 7A). This observation indicates that one functional ankyrin-G-interaction domain is sufficient for targeting KCNQ2/3 to the AIS and demonstrates the importance of an examination of the behavior of the heteromeric complex when analyzing BFNC mutations. Indeed, our data indicate that a BFNC KCNQ2 mutation, the P681-frameshift mutation, which abolishes KCNQ2/3 expression at the axonal cell surface (Chung et al., 2006; Coppola et al., 2003) possibly does so by the replacement of the distal C-terminal sequences or by factors upstream of the ankyrin-G-binding motif rather than by deleting the ankyrin-G-binding motif itself.

Furthermore, KCNQ3 subunits can also interact with other members of the KCNQ potassium channel family, namely KCNQ4 and KCNQ5 (Kubisch et al., 1999; Schroeder et al., 2000). KCNQ5 subunits are also expressed in hippocampal pyramidal neurons (Shah et al., 2002). As only one ankyrin-G-interaction motif is required for AIS localization, KCNQ3/5 complexes could potentially also localize to the AIS through the motif contained within KCNQ3 subunits. Whether this is the case or KCNQ5 subunits localize differently in hippocampal neurons will be an interesting subject for future study.

## Materials and Methods

### Cell cultures

Hippocampal cultures were prepared as previously described (Banker and Cowan, 1977) with modifications. Briefly, hippocampi from 19-day rat embryos of pregnant Wistar rats were dissociated by treatment with trypsin (0.25% w/v) for 15 minutes at 37°C followed by triturating with a constricted Pasteur pipet. The cells were plated on glass coverslips coated with 1 mg/ml poly-L-lysine at ≈10,000 cells/cm$^2$ in minimal essential medium (MEM; Invitrogen) supplemented with 10% horse serum, 0.06% glucose, and 10 IU/ml penicillin-streptomycin. After 2-4 hours, when the cells were adhered to the substrate, the coverslips were transferred into six-well tissue culture plates containing a confluent layer of glial cells. Glial cell suspensions obtained from rat embryonic hippocampi at E19 were plated at 5000 cells/cm$^2$ and grown for 2-3 weeks to confluence in minimal essential medium (MEM; Invitrogen) supplemented with 10% horse serum, 0.6% glucose, and 10 IU/ml penicillin-streptomycin. Neurons were grown on the astroglial feeder layer in serum-free neurobasal medium supplemented with B27 (Invitrogen). After 3 days, 5 μM cytosine arabinoside was added to inhibit the proliferation of non-neuronal cells. Cultures were kept at 37°C in a humidified atmosphere of 95% air and 5% $CO_2$. One half of the culture medium was changed weekly.

### Reverse-transcription PCR (RT-PCR)

RT-PCR was performed on cultured hippocampal neurons at 10 days in vitro (DIV), the time at which transfected cells were analyzed for exogenous expression of KCNQ proteins. RNA from three independent cultures was tested. Total RNA was extracted from hippocampal neurons grown in 60 mm dishes (at 12,000 cells/cm$^2$) (Misonou and Trimmer, 2005), treated with DNase I using the RNeasy mini system (Qiagen) and reverse transcribed using an anchored poly-T primer (T24-V-N) and SuperScript™ III (Invitrogen). The RT product was subjected to PCR amplification

using oligodeoxynucleotide primers based on rat sequences (GenBank accession nos: KCNQ1, NM032073; KCNQ2, NM133322; KCNQ3, NM031597; KCNQ4, AF249748; KCNQ5, XM237012). All primers for amplification of rKCNQs were designed to be exon spanning with $T_m$ of 68-70°C and were as follows:
rKCNQ1 (1525s): CACCATCGGGCCACCATCAAGGTCATC;
rKCNQ1 (1763a): GATGGTGTTGCTGCCACGGTCTTTGCTCTT;
rKCNQ2 (1536s): TGAAGATCTTACCCCTGGCCTCAAAGTCAGC;
rKCNQ2 (1769a): GCCTTTGGTGCGGTCCTTGTCCGTTATTG;
rKCNQ3 (1531s): GACATGATCCCCACCCTAAAGGCTGCCA;
rKCNQ3 (1770a): CTGACCCTTTCTGAGACTTCTTATGTTTTGGAGTGGAT;
rKCNQ4 (256s): GGTGGATGATGTCATGCCTGCTGTGAAGA;
rKCNQ4 (498a): ACCCTTATCGCCCTTCTCCCGAGTCTTG;
rKCNQ5 (1612s): CTCAAAACCGTCATCCGAGCCATCAGAATCA;
rKCNQ5 (1846a): GTCTCGTGTTCTGCTGTTATTTTCTCTCGGCTCTT.

The cycling conditions used were: 1 cycle at 97°C for 2 minutes; 30 cycles at 97°C for 30 seconds, 56°C for 30 seconds, 72°C for 1 minute; 1 cycle at 72°C for 5 minute. Amplified products were analyzed by electrophoresis on 2% agarose gels.

## Plasmids and cloning

Expression of human KCNQ2 (hKCNQ2) and human KCNQ3 (hKCNQ3) was obtained by the use of plasmid pCMV-KCNQ2-cmyc and pCMV-KCNQ3-FLAG, respectively. The constructs hKCNQ2delAnkG (Δ803-844) and hKCNQ3-delAnkG (Δ826-872) were constructed using standard PCR techniques and subsequently cloned into the pcDNA3.1 vector for expression in mammalian cells. The constructs KCNQ2-E810A/S811A/D812A (KCNQ2-AAA) and KCNQ3-E837A/T838A/D839A (KCNQ3-AAA) were generated using the QuikChange Site-Directed Mutagenesis Kit (Stratagene).

## Neuron transfection

Cultured hippocampal neurons at 7-8 days DIV were transfected by the LipofectAMINE 2000 method (Invitrogen). Briefly, 0.9 μg of DNA (0.3 μg of each KCNQ construct and empty vector to total 0.9 μg) was mixed with 50 μl of MEM medium (Invitrogen). In another tube, 2 μl of Lipofectamine2000 was mixed with 50 μl of MEM and incubated for 5 minutes. DNA and Lipofectamine 2000 were mixed, incubated and added to face-up coverslips in individual wells of 6-well tissue culture plates containing Neurobasal medium supplemented with 0.25 mM L-glutamine. Transfection was carried out for 1 hour at 37°C, 5% $CO_2$, after which the neurons were transferred back to the dishes containing the glial cell layer. Neurons were left for expression for 48 hours.

## Electrophysiological recordings

Whole-cell patch clamp experiments were performed to obtain voltage clamp or current clamp recordings from cultured, transfected hippocampal neurons at room temperature essentially as described previously (Shahidullah et al., 2005). Pyramidal cells were selected based on morphology and ability to elicit action potentials under current clamp conditions. The extracellular solution contained: 120 mM NaCl, 3 mM KCl, 2.5 mM $CaCl_2$, 1.2 mM $MgCl_2$, 11 mM glucose, 5 mM HEPES, 23 mM $NaHCO_3$ (pH 7.4 with HCl). After action potential generation, the extracellular solution was switched to a solution containing 1 μM tetrodotoxin to minimize $Na^+$ currents. The internal solution contained: 160 mM K-acetate, 3 mM $MgCl_2$, 2 mM $K_2ATP$ and 20 mM HEPES (pH 7.4 with KOH). Borosilicate glass pipettes were pulled on a DMZ Universal electrode puller (Zeitz Instruments, Germany) to a resistance of 2-3 MΩ when filled with internal solution. Under these conditions, after an initial fast run-down, voltage clamp current remained stable for at least 10 minutes within which all measurements were completed. Series resistance was measured continuously throughout experiments, kept below 10 MΩ and compensated for at 80% automatically by the acquisition software Pulse (HEKA Instruments, Germany). Patch-clamp experiments were performed with a HEKA EPC-9 patch clamp amplifier (HEKA instruments, Germany) on an inverted Olympus IX-70 microscope (Olympus instruments, Germany). Data was acquired at a 5 kHz sampling rate. At 5-second intervals, cells were depolarized to –20 mV for 500 ms and M-currents were subsequently recorded at either –40 mV for 500 ms (continuous recordings) or over a range of voltages (before and after drug application). Cells were held at –70 mV between recording intervals.

### Data analysis

The M-current for a given cell was measured by determining the difference current at –40 mV before and after application of 10 μM XE-991. Means were compared statistically with a one-way analysis of variance. Individual means were compared to the control condition with Dunnet's post-hoc test. The time course of current shows total whole-cell, leak subtracted current measured at –40mV, which has a residual 10 μM XE-991 insensitive current.

## Immunofluorescence

Neurons (10 and 21 DIV) were fixed with 4% paraformaldehyde/4% sucrose in PBS (pH 7.4) for 20 minutes at 4°C. Quenching was performed by 30-minute incubation with 0.1% Triton X-100/4% milk in TBS (wash buffer). The cells were then incubated for 1 hour in primary antibody diluted in wash buffer. Primary antibodies employed were: a monoclonal anti-MAP2 (1:1000, clone HM-2, Sigma Aldrich); a mouse monoclonal anti-protein disulfide isomerase (PDI) (1:250, clone 1D3, Nordic Biosite, Täby, Sweden); a monoclonal mouse anti-ankyrin-G (1:15, clone 4G3F8), a polyclonal goat anti-KCNQ3 (1:20) and a polyclonal rabbit anti-cmyc tag (1:50) (Santa Cruz Biotechnology, Heidelberg, Germany); a polyclonal rabbit anti-KCNQ3 (1:100, Alomone Labs, Jerusalem, Israel); and a polyclonal rabbit anti-KCNQ2 antibody [1:50 (endogenous) or 1:500 (exogenous), Affinity BioReagents]. For double and triple labeling all primary antibodies were applied simultaneously. Secondary antibodies were diluted in wash buffer and applied for 45 minutes. As secondary antibodies an Alexa™Fluor 488 goat anti-mouse antibody (1:800), an Alexa™Fluor 568 goat anti-rabbit (1:800), an Alexa™Fluor 488 donkey anti-mouse (1:200), an Alexa™Fluor 568 donkey anti-goat antibody (1:800), an Alexa™Fluor 488 donkey anti-rabbit antibody (1:300) and an Alexa™Fluor 647 chicken anti-mouse (1:300) all from Invitrogen were employed. After washing the labeled cells were mounted in Prolong Gold (Invitrogen).

## Quantification

Determination of the AIS/distal axon and AIS/dendrite ratios was performed essentially as described (Chung et al., 2006; Gu et al., 2003). The mean fluorescence intensity of the axon within 30 μm of the soma (AIS), at 60-90 μm from the soma (distal axon) or in major dendrites at 20-50 μm from the soma (dendrites) was measured using the Leica confocal software and subtracted for background fluorescence (the mean intensity of the background was obtained from an area of the image absent of neurons or processes).

### Data analysis

For each construct 20-30 cells from 2-4 independent cultures were measured. Means were compared statistically with a one-way analysis of variance followed by a Bonferroni comparison of selected pairs.

## Fluorescence immunohistochemistry

Male adult Wistar rats were anesthetized with tri-brome ethanol and intracardially perfused with 4% paraformaldehyde (PFA) in PBS (pH 7.4). The brain was removed and postfixed overnight at 4°C in 4% PFA. The tissue was dehydrated and embedded in paraffin and 5 μm thick sections were cut. The sections were rehydrated in a toluene-ethanol series and microwave oven-heated in a 10 mmol/L citric acid buffer. The sections were washed in PBS and incubated for 30 minutes in blocking buffer (0.2% fish skin gelatin, 0.1% Triton X-100 in PBS). They were subsequently incubated with the primary antibodies (rabbit anti-KCNQ2, 1:50, rabbit anti-KCNQ3, 1:100, mouse anti-ankyrin-G 1:15) overnight at 4°C. Ankyrin-G staining was amplified using a biotinylated donkey anti-mouse antibody (1:500, Jackson Immunoresearch Laboratories, Westgrove, PA) for 1 hour at room temperature. Secondary antibody (Alexa®Fluor 568 goat anti-rabbit, 1:800, Invitrogen) and Alexa®Fluor 488-coupled streptavidin (1:200, Invitrogen) were then applied for 1 hour at room temperature. Sections were mounted in Prolong Gold (Invitrogen).

## Confocal microscopy and imaging

Laser scanning confocal microscopy was performed using the Leica TCS SP2 system equipped with argon and helium-neon lasers. The objective was 63× W, NA 1.2. For double-and triple-labeling experiments sequential scanning was employed to allow separation of signals from the channels. Images were treated using Adobe Photoshop 5.5 and Adobe Illustrator 9.0.

## Immunoblot analysis

Purified rat brain membranes (30 μg/lane) and total lysates of primary hippocampal neurons were separated on 4-15% SDS-PAGE polyacrylamide gels using the Bio-Rad Laboratories minigel system (Hercules, CA). Proteins were transferred onto a hybond-P PVDF transfer membrane (Amersham Biosciences, 0.45 μm) in 25 mM Tris base, 200 mM glycine, 20% methanol using a mini transblot (Hercules, CA). After transfer, the membranes were incubated for 1 hour at room temperature in blocking buffer (PBS containing 4% low-fat milk powder). The membrane was incubated overnight at room temperature in blocking buffer containing primary antibodies [rabbit anti-KCNQ2, 1:800 dilution (Affinity BioReagents), rabbit anti-KCNQ3, 1:200 (Alomone Labs, Jerusalem, Israel), rabbit anti-ankyrin-G, 1:75 (Santa Cruz Biotechnology, Heidelberg, Germany)]. After washing, bound antibody was revealed with HRP-conjugated donkey anti-rabbit antibody (1/10,000, Jackson Immunosearch Laboratories) in blocking buffer for 45 minutes, followed by visualization with the Supersignal West Pico Chemiluminescent detection system (Pierce) according to the manufacturer's instructions. Immunoblots were exposed on hyperfilm ECL (Amersham Biosciences).

The Lundbeck Foundation, The Danish Medical Research Council, Fonden af 17.12.1981, The Velux Foundation, the Novo Nordisk Foundation and the American Heart Association supported this work. We thank Pia Hagman and Inge Kjeldsen for excellent technical assistance.

## References


**Banker, G. A. and Cowan, W. M.** (1977). Rat hippocampal neurons in dispersed cell culture. *Brain Res.* **126**, 397-442.

**Biervert, C., Schroeder, B. C., Kubisch, C., Berkovic, S. F., Propping, P., Jentsch, T. J. and Steinlein, O. K.** (1998). A potassium channel mutation in neonatal human epilepsy. *Science* **279**, 403-406.

**Brown, D. A. and Adams, P. R.** (1980). Muscarinic suppression of a novel voltage-sensitive K+ current in a vertebrate neurone. *Nature* **283**, 673-676.

**Catterall, W. A.** (1981). Localization of sodium channels in cultured neural cells. *J. Neurosci.* **1**, 777-783.

**Charlier, C., Singh, N. A., Ryan, S. G., Lewis, T. B., Reus, B. E., Leach, R. J. and Leppert, M.** (1998). A pore mutation in a novel KQT-like potassium channel gene in an idiopathic epilepsy family. *Nat. Genet.* **18**, 53-55.

**Chung, H. J., Jan, Y. N. and Jan, L. Y.** (2006). Polarized axonal surface expression of neuronal KCNQ channels is mediated by multiple signals in the KCNQ2 and KCNQ3 C-terminal domains. *Proc. Natl. Acad. Sci. USA* **103**, 8870-8875.

**Colino, A. and Halliwell, J. V.** (1987). Differential modulation of three separate K-conductances in hippocampal CA1 neurons by serotonin. *Nature* **328**, 73-77.

**Cooper, E. C., Aldape, K. D., Abosch, A., Barbaro, N. M., Berger, M. S., Peacock, W. S., Jan, Y. N. and Jan, L. Y.** (2000). Colocalization and coassembly of two human brain M-type potassium channel subunits that are mutated in epilepsy. *Proc. Natl. Acad. Sci. USA* **97**, 4914-4919.

**Cooper, E. C., Harrington, E., Jan, Y. N. and Jan, L. Y.** (2001). M channel KCNQ2 subunits are localized to key sites for control of neuronal network oscillations and synchronization in mouse brain. *J. Neurosci.* **21**, 9529-9540.

**Coppola, G., Castaldo, P., Miraglia del Giudice, E., Bellini, G., Galasso, F., Soldovieri, M. V., Anzalone, L., Sferro, C., Annunziato, L., Pascotto, A. et al.** (2003). A novel KCNQ2 K+ channel mutation in benign neonatal convulsions and centrotemporal spikes. *Neurology* **61**, 131-134.

**Cruzblanca, H., Koh, D. S. and Hille, B.** (1998). Bradykinin inhibits M current via phospholipase C and Ca2+ release from IP3-sensitive Ca2+ stores in rat sympathetic neurons. *Proc. Natl. Acad. Sci. USA* **95**, 7151-7156.

**Davis, J. Q. and Bennett, V.** (1994). Ankyrin binding activity shared by the neurofascin/L1/NrCAM family of nervous system cell adhesion molecules. *J. Biol. Chem.* **269**, 27163-27166.

**Delmas, P. and Brown, D. A.** (2005). Pathways modulating neural KCNQ/M (Kv7) potassium channels. *Nat. Rev. Neurosci.* **6**, 850-862.

**Devaux, J. J., Kleopa, K. A., Cooper, E. C. and Scherer, S. S.** (2004). KCNQ2 is a nodal K+ channel. *J. Neurosci.* **24**, 1236-1244.

**Etxeberria, A., Santana-Castro, I., Regalado, M. P., Aivar, P. and Villarroel, A.** (2004). Three mechanisms underlie KCNQ2/3 heteromeric potassium M-channel potentiation. *J. Neurosci.* **24**, 9146-9152.

**Garrido, J. J., Giraud, P., Carlier, E., Fernandes, F., Moussif, A., Fache, M. P., Debanne, D. and Dargent, B.** (2003). A targeting motif involved in sodium channel clustering at the axonal initial segment. *Science* **300**, 2091-2094.

**Geiger, J., Weber, Y. G., Landwehrmeyer, B., Sommer, C. and Lerche, H.** (2006). Immunohistochemical analysis of KCNQ3 potassium channels in mouse brain. *Neurosci. Lett.* **400**, 101-104.

**Gu, C., Jan, Y. N. and Jan, L. Y.** (2003). A conserved domain in axonal targeting of Kv1 (Shaker) voltage-gated potassium channels. *Science* **301**, 646-649.

**Jenkins, S. M. and Bennett, V.** (2001). Ankyrin-G coordinates assembly of the spectrin-based membrane skeleton, voltage-gated sodium channels, and L1 CAMs at Purkinje neuron initial segments. *J. Cell Biol.* **155**, 739-746.

**Kordeli, E., Lambert, S. and Bennett, V.** (1995). AnkyrinG. A new ankyrin gene with neural-specific isoforms localized at the axonal initial segment and node of Ranvier. *J. Biol. Chem.* **270**, 2352-2359.

**Kubisch, C., Schroeder, B. C., Friedrich, T., Lutjohann, B., El Amraoui, A., Marlin, S., Petit, C. and Jentsch, T. J.** (1999). KCNQ4, a novel potassium channel expressed in sensory outer hair cells, is mutated in dominant deafness. *Cell* **96**, 437-446.

**Lemaillet, G., Walker, B. and Lambert, S.** (2003). Identification of a conserved ankyrin-binding motif in the family of sodium channel alpha subunits. *J. Biol. Chem.* **278**, 27333-27339.

**Misonou, H. and Trimmer, J. S.** (2005). A primary culture system for biochemical analyses of neuronal proteins. *J. Neurosci. Methods* **144**, 165-173.

**Pan, Z., Kao, T., Horvath, Z., Lemos, J., Sul, J. Y., Cranstoun, S. D., Bennett, V., Scherer, S. S. and Cooper, E. C.** (2006). A common ankyrin-G-based mechanism retains KCNQ and NaV channels at electrically active domains of the axon. *J. Neurosci.* **26**, 2599-2613.

**Peters, H. C., Hu, H., Pongs, O., Storm, J. F. and Isbrandt, D.** (2005). Conditional transgenic suppression of M channels in mouse brain reveals functions in neuronal excitability, resonance and behavior. *Nat. Neurosci.* **8**, 51-60.

**Roche, J. P., Westenbroek, R., Sorom, A. J., Hille, B., Mackie, K. and Shapiro, M. S.** (2002). Antibodies and a cysteine-modifying reagent show correspondence of M current in neurons to KCNQ2 and KCNQ3 K+ channels. *Br. J. Pharmacol.* **137**, 1173-1186.

**Schroeder, B. C., Kubisch, C., Stein, V. and Jentsch, T. J.** (1998). Moderate loss of function of cyclic-AMP-modulated KCNQ2/KCNQ3 K+ channels causes epilepsy. *Nature* **396**, 687-690.

**Schroeder, B. C., Hechenberger, M., Weinreich, F., Kubisch, C. and Jentsch, T. J.** (2000). KCNQ5, a novel potassium channel broadly expressed in brain, mediates M-type currents. *J. Biol. Chem.* **275**, 24089-24095.

**Schwake, M., Pusch, M., Kharkovets, T. and Jentsch, T. J.** (2000). Surface expression and single channel properties of KCNQ2/KCNQ3, M-type K+ channels involved in epilepsy. *J. Biol. Chem.* **275**, 13343-13348.

**Schwarz, J. R., Glassmeier, G., Cooper, E., Kao, T., Nodera, H., Tabuena, D., Kaji, R. and Bostock, H.** (2006). KCNQ channels mediate IKs, a slow K+ current regulating excitability in the node of Ranvier. *J. Physiol.* **573**, 17-34.

**Shah, M. M., Mistry, M., Marsh, S. J., Brown, D. A. and Delmas, P.** (2002). Molecular correlates of the M-current in cultured rat hippocampal neurons. *J. Physiol.* **544**, 29-37.

**Shahidullah, M., Santarelli, L. C., Wen, H. and Levitan, I. B.** (2005). Expression of a calmodulin-binding KCNQ2 potassium channel fragment modulates neuronal M-current and membrane excitability. *Proc. Natl. Acad. Sci. USA* **102**, 16454-16459.

**Shapiro, M. S., Wollmuth, L. P. and Hille, B.** (1994). Angiotensin II inhibits calcium and M current channels in rat sympathetic neurons via G proteins. *Neuron* **12**, 1319-1329.

**Simmons, M. A., Schneider, C. R. and Krause, J. E.** (1994). Regulation of the responses to gonadotropin-releasing hormone, muscarine and substance P in sympathetic neurons by changes in cellular constituents and intracellular application of peptide fragments of the substance P receptor. *J. Pharmacol. Exp. Ther.* **271**, 581-589.

**Singh, N. A., Charlier, C., Stauffer, D., DuPont, B. R., Leach, R. J., Melis, R., Ronen, G. M., Bjerre, I., Quattlebaum, T., Murphy, J. V. et al.** (1998). A novel potassium channel gene, KCNQ2, is mutated in an inherited epilepsy of newborns. *Nat. Genet.* **18**, 25-29.

**Wang, H. S., Pan, Z., Shi, W., Brown, B. S., Wymore, R. S., Cohen, I. S., Dixon, J. E. and McKinnon, D.** (1998). KCNQ2 and KCNQ3 potassium channel subunits: molecular correlates of the M-channel. *Science* **282**, 1890-1893.

**Watanabe, H., Nagata, E., Kosakai, A., Nakamura, M., Yokoyama, M., Tanaka, K. and Sasai, H.** (2000). Disruption of the epilepsy KCNQ2 gene results in neural hyperexcitability. *J. Neurochem.* **75**, 28-33.

**Weber, Y. G., Geiger, J., Kampchen, K., Landwehrmeyer, B., Sommer, C. and Lerche, H.** (2006). Immunohistochemical analysis of KCNQ2 potassium channels in adult and developing mouse brain. *Brain Res.* **1077**, 1-6.

**Zhou, D., Lambert, S., Malen, P. L., Carpenter, S., Boland, L. M. and Bennett, V.** (1998). AnkyrinG is required for clustering of voltage-gated Na channels at axon initial segments and for normal action potential firing. *J. Cell Biol.* **143**, 1295-1304.